

Truncated Variational Sampling for ‘Black Box’ Optimization of Generative Models

Jörg Lücke

joerg.luecke@uol.de
Universität Oldenburg and
Cluster of Excellence H4a
Oldenburg, Germany

Zhenwen Dai

zhenwend@amazon.com
Amazon Research
Cambridge, UK

Georgios Exarchakis

georgios.exarchakis@ens.fr
Department d’Informatique
École Normale Supérieure
Paris, France

Abstract

We investigate the optimization of two generative models with binary hidden variables using a novel variational EM approach. The novel approach distinguishes itself from previous variational approaches by using hidden states as variational parameters. Here we use efficient and general purpose sampling procedures to vary the hidden states, and investigate the ‘black box’ applicability of the resulting optimization procedure. For general purpose applicability, samples are drawn from approximate marginal distributions of the considered generative model and from the prior distribution of a given generative model. As such, sampling is defined in a generic form with no additional derivations required. As a proof of concept, we then apply the novel procedure (A) to Binary Sparse Coding (a model with continuous observables), and (B) to basic Sigmoid Belief Networks (which are models with binary observables). The approach is applicable without any further analytical steps and efficiently as well as effectively increases the variational free-energy objective.

1 Introduction

The use of expectation maximization (EM; Dempster et al., 1977) for advanced probabilistic data models requires approximations because EM with an exact E-step (computing the full posterior) is typically intractable. Many models of recent interest have binary latents (Goodfellow et al., 2012; Gan et al., 2015; Dai and Lücke, 2014; Mnih and Gregor, 2014; Sheikh et al., 2014; Sheikh and Lücke, 2016), and for such models these intractabilities are primarily computa-

tional: exact E-steps can be computed but they scale exponentially with the number of latents. To overcome intractabilities, efficiently computable approximation methods for EM have been developed. For models with binary latents there are typically two types of approaches applied: sampling approaches or variational EM with the latter having been dominated by factored variational approaches in the past (e.g. Jordan et al., 1999; MacKay, 2003). Variational approaches and sampling have also often been combined (Shelton et al., 2011; Hoffman et al., 2013; Salimans et al., 2015; Hernandez-Lobato et al., 2016; Sheikh and Lücke, 2016) to leverage the advantages of both methods. Given a generative model, both sampling and variational EM require often cumbersome derivations either to derive efficient posterior samplers or to derive update equations for variational parameter optimization. The question how procedures can be defined that automatize the development of learning algorithms for generative models to avoid these additional efforts, has therefore shifted into the focus of recent research (Ranganath et al., 2014; Tran et al., 2015; Rezende and Mohamed, 2015; Kucukelbir et al., 2016; Hernandez-Lobato et al., 2016; Shelton et al., 2017).

In this paper we make use of novel theoretical results (Lücke, 2016) to couple variational EM and sampling exceptionally tightly. We then show how such a coupling can be used to define a ‘black box’ optimization procedure for generative models with binary latents. Our approach is based on truncated posteriors as variational distributions. Truncated approximations have been studied previously (Lücke and Eggert, 2010; Shelton et al., 2011; Bornschein et al., 2013; Dai and Lücke, 2014; Sheikh et al., 2014; Sheikh and Lücke, 2016) but required the definition of appropriate preselection mechanisms for a given generative model. In contrast,

we here use samples drawn from model dependent distributions to directly define truncated variational distributions, and the samples themselves act as variational parameters.

2 Truncated Posteriors and Sampling

Let us consider generative models with H binary latent variables, $\vec{s} = (s_1, \dots, s_H)$ with $s_h \in \{0, 1\}$. Truncated approximations have been motivated by the observation that the exponentially large sums over states required for expectation values w.r.t. posteriors are typically dominated by summands corresponding to very few states. If for a given data point $\vec{y}^{(n)}$ these few states are contained in a set $\mathcal{K}^{(n)}$, we can define a posterior approximation as follows (compare Lücke and Eggert, 2010; Sheikh et al., 2014):

$$q^{(n)}(\vec{s}; \mathcal{K}, \Theta) = \frac{p(\vec{s} | \vec{y}^{(n)}, \Theta) \delta(\vec{s} \in \mathcal{K}^{(n)})}{\sum_{\vec{s}' \in \mathcal{K}^{(n)}} p(\vec{s}' | \vec{y}^{(n)}, \Theta)}, \quad (1)$$

where $\delta(\vec{s} \in \mathcal{K}^{(n)}) = 1$ if $\mathcal{K}^{(n)}$ contains \vec{s} and zero otherwise. It is straight-forward to derive expectation values w.r.t. these approximate posteriors simply by inserting (1) into the definition of expectation values and by multiplying numerator and denominator by $p(\vec{y}^{(n)} | \Theta)$, which yields:

$$\langle g(\vec{s}) \rangle_{q^{(n)}} = \frac{\sum_{\vec{s} \in \mathcal{K}^{(n)}} p(\vec{s}, \vec{y}^{(n)} | \Theta) g(\vec{s})}{\sum_{\vec{s}' \in \mathcal{K}^{(n)}} p(\vec{s}', \vec{y}^{(n)} | \Theta)} \quad (2)$$

where $g(\vec{s})$ is a function of the hidden variables. As the dominating summands are different for each data point $\vec{y}^{(n)}$, the sets $\mathcal{K}^{(n)}$ are different. If a set $\mathcal{K}^{(n)}$ now contains those states \vec{s} which dominate the sums over the joints w.r.t. the exact posterior, then Eqn. 2 is a very accurate approximation.

Truncated posterior approximations have successfully been applied to a number of elementary and more advanced generative models (e.g. Henniges et al., 2014; Sheikh et al., 2014; Shelton et al., 2017), and they do not suffer from potential biases introduced by posterior independence assumptions made by factored variational approximations (Ilin and Valpola, 2005; Turner and Sahani, 2011; Sheikh et al., 2014). Previously, the sets $\mathcal{K}^{(n)}$ were defined based on sparsity assumptions (Lücke and Sahani, 2008) or based on sparsity and latent preselection (Lücke and Eggert, 2010; Shelton et al., 2017). The approach followed here, in contrast, uses sets $\mathcal{K}^{(n)}$ which contain samples from model

and data dependent distributions. By treating the truncated distribution (1) as variational distributions within a free-energy framework (Lücke, 2016), we can then derive efficient procedures to update the samples in $\mathcal{K}^{(n)}$ such that the variational free-energy is always monotonically increased.

For this we use the following theoretical results (see Suppl. A for details): (1) We use that the M-step equations remain unchanged if instead of exact posteriors the truncated posteriors (1) are used; (2) We make use of the result that after each M-step the free-energy corresponding to truncated variational distributions is given by the following simplified and computationally tractable form:

$$\mathcal{F}(\mathcal{K}, \Theta) = \sum_n \log \left(\sum_{\vec{s} \in \mathcal{K}^{(n)}} p(\vec{s}, \vec{y}^{(n)} | \Theta) \right), \quad (3)$$

where $\mathcal{K} = (\mathcal{K}^{(1)}, \dots, \mathcal{K}^{(N)})$. The variational E-step then consists of finding a set \mathcal{K}_{new} which increases $\mathcal{F}(\mathcal{K}, \Theta)$ w.r.t. \mathcal{K} . The M-step consist of the standard M-step equations but with expectation values estimated by (2).

For mixture models, a full E-step can be realized in which the objective function (3) is maximized w.r.t. \mathcal{K} after exhaustively computing latent states (Forster and Lücke 2017; Lücke and Forster 2017, also compare Hughes and Sudderth 2016). For multiple-cause models we here seek to find new sets $\tilde{\mathcal{K}}$ using sampling, such that the free-energy is increased, $\mathcal{F}(\tilde{\mathcal{K}}, \Theta) > \mathcal{F}(\mathcal{K}, \Theta)$, (which corresponds to a partial E-step). To keep the computational demand limited, we will take the sets \mathcal{K} and $\tilde{\mathcal{K}}$ to be of constant size after each E-step by demanding $|\mathcal{K}^{(n)}| = |\tilde{\mathcal{K}}^{(n)}| = S$ for all n .

Instead of explicitly computing and comparing the free-energies (3) w.r.t. \mathcal{K} and $\tilde{\mathcal{K}}$, we can instead use a comparison of joint probabilities $p(\vec{s}, \vec{y}^{(n)} | \Theta)$ as a criterion for free-energy increase. The following can be shown:

For a replacement of $\vec{s} \in \mathcal{K}^{(n)}$ by a new state $\vec{s}_{\text{new}} \notin \mathcal{K}^{(n)}$ the free-energy $\mathcal{F}(\mathcal{K}, \Theta)$ is increased if and only if

$$p(\vec{s}_{\text{new}}, \vec{y}^{(n)} | \Theta) > p(\vec{s}, \vec{y}^{(n)} | \Theta). \quad (4)$$

Criterion (4) may directly be concluded by considering the functional form of Eqn. 3 (see Lücke, 2016, for a formal proof). It means that the free-energy is guaranteed to increase if we replace, e.g., the state with the lowest joint in $\mathcal{K}^{(n)}$ by a newly sampled state $\vec{s}_{\text{new}} \notin \mathcal{K}^{(n)}$ with a higher joint. Instead of comparing single joints, a computationally more efficient procedure is to use batches of many newly sampled states, and then to use criterion (4) to increase $\mathcal{F}(\mathcal{K}, \Theta)$ as

Algorithm 1: Sampling-based Variational E-step

for $n = 1, \dots, N$ do

draw M samples $\vec{s} \sim p_{\text{var}}^{(n)}(\vec{s})$; define $\mathcal{K}_{\text{new}}^{(n)}$ to contain all M samples; set $\mathcal{K}^{(n)} = \mathcal{K}^{(n)} \cup \mathcal{K}_{\text{new}}^{(n)}$; remove those $(\mathcal{K}^{(n)} - S)$ samples \vec{s} in $\mathcal{K}^{(n)}$ with the lowest $p(\vec{s}, \vec{y}^{(n)} \Theta)$;
--

much as possible. Such a procedure is given by Alg. 1: For each data point n , we first draw M new samples from a yet to be specified distribution $p_{\text{var}}^{(n)}(\vec{s})$. These samples are then united with the states already in $\mathcal{K}^{(n)}$. Of this union of old and new states, we then take the S states with highest joints to define the new state set $\mathcal{K}^{(n)}$. This last step selects because of (4) the best possible subset of the union (see Suppl. B). Furthermore, selecting the S states with largest joints represents a standard unsorted partial sorting problem which is solvable in linear time complexity (Blum et al., 1973), i.e., with at most $\mathcal{O}(M + S)$ in our case (see Suppl. B). Equivalently to selecting the S largest joints, we can also remove the $(|\mathcal{K}^{(n)}| - S)$ lowest joints (which is the last line in Alg. 1). For *any* distribution $p_{\text{var}}^{(n)}(\vec{s})$, Alg. 1 is guaranteed to monotonously increase the free-energy $\mathcal{F}(\mathcal{K}, \Theta)$ w.r.t. \mathcal{K} .

3 Posterior, Prior & Marginal Sampling

While the partial E-step of Alg. 1 monotonously increases the free-energy for any distribution $p_{\text{var}}^{(n)}(\vec{s})$ used for sampling, the specific choice for $p_{\text{var}}^{(n)}(\vec{s})$ is of central importance for the efficiency of the procedure. If the distribution is not chosen well, any significant increase of $\mathcal{F}(\mathcal{K}, \Theta)$ may require unreasonable amounts of time, e.g., because new samples which increase $\mathcal{F}(\mathcal{K}, \Theta)$ are sampled too infrequently. By considering Alg. 1, the requirement for $p_{\text{var}}^{(n)}(\Theta)$ is to provide samples with high joint probability $p(\vec{s}, \vec{y}^{(n)} | \Theta)$ for a given $\vec{y}^{(n)}$. The first distribution that comes to mind for $p_{\text{var}}^{(n)}(\Theta)$ is the posterior distribution $p(\vec{s} | \vec{y}^{(n)}, \Theta)$. Samples from the posterior are likely to have high posterior mass and therefore high joint mass relative to the other states because all states share the same normalizer $p(\vec{y}^{(n)} | \Theta)$. On the downside, however, sampling from the posterior may not be an easy task for models with binary latents and a relatively high dimensionality as we intend to aim at here. Furthermore, the deriva-

tion of posterior samplers requires additional analytical efforts for any new generative model we apply the procedure to, and requires potentially additional design choices such as definitions of proposal distributions. All these points are contrary to our goal of a ‘black box’ procedure which is applicable as generally and generically as possible. Instead, we therefore seek distributions $p_{\text{var}}^{(n)}(\Theta)$ for Alg. 1 that can efficiently optimize the free-energy but that can be defined without requiring model-specific analytical derivations. Candidates for $p_{\text{var}}^{(n)}(\Theta)$ are consequently the prior distribution of the given generative model, $p(\vec{s} | \Theta)$, or the marginal distribution.

A prior sampler is usually directly given by the generative model but may have the disadvantage that finally new samples only very rarely increase the free-energy because the prior sampler is independent of a given data point (only the average over data points has high posterior mass). Marginal samplers, on the other hand, are data driven but the computation of activation probabilities $p(s_h = 1 | \vec{y}^{(n)}, \Theta)$ is unfortunately not computationally efficient. To obtain data-driven but efficient samplers, we will for our purposes, therefore, use approximate marginal samplers.

1st Approximation. First observe that we can obtain an efficiently computable approximation to a marginal sampler by using the truncated distributions $q^{(n)}(\vec{s})$ in (1) themselves. For binary latents s_h we can approximate:

$$p(s_h = 1 | \vec{y}^{(n)}, \Theta) = \langle s_h \rangle_{p(\vec{s} | \vec{y}^{(n)}, \Theta)} \approx \langle s_h \rangle_{q^{(n)}(\vec{s})}. \tag{5}$$

and accordingly $p(s_h = 0 | \vec{y}^{(n)}, \Theta)$. Because of the arguments given above the expectations (2) w.r.t. $q^{(n)}(\vec{s})$ are efficiently computable and are given by:

$$\langle s_h \rangle_{q^{(n)}(\vec{s})} = \frac{\sum_{\vec{s} \in \mathcal{K}^{(n)}} p(\vec{s}, \vec{y}^{(n)} | \Theta) s_h}{\sum_{\vec{s}' \in \mathcal{K}^{(n)}} p(\vec{s}', \vec{y}^{(n)} | \Theta)} \tag{6}$$

Using Eqn. 5 with Eqn. 6 we can consequently define for each latent h an approximation of the marginal $p(s_h = 1 | \vec{y}^{(n)}, \Theta)$. Given a directed generative model, no derivations are required to efficiently generate samples from this approximation because the joint probabilities of Eqn. 6 can directly be computed. The truncated marginal sampler defined by Eqn. 5 becomes increasingly similar to an exact marginal sampler the better the truncated distributions approximate the exact posteriors.

2nd Approximation. To further improve efficiency and convergence times, we optionally apply a second

approximation by using the approximate marginal distributions (Eqns. 5 and 6) as target objective for a parametric function $f_h(\bar{y}^{(n)}; \Lambda)$ which approximates the truncated marginal. A parametric function from data to marginal probabilities of the latents has the advantage of modeling data similarities by mapping similar data to similar marginal distributions. The mapping incorporates information across the data points, which can facilitate training and, e.g., avoids more expensive $\mathcal{K}^{(n)}$ updates of some data points due to bad initialization. The mapping $f_h(\bar{y}^{(n)}; \Lambda)$ is estimated with the training data and the current approximate marginal $q_{\text{mar}}(s_h = 1 | \bar{y}, \Theta)$ defined by (5) and (6). For simplicity, we use a Multi-Layer Perceptron (MLP) for the function mapping and trained with cross-entropy. We use a generic MLP with one hidden layer. As such, the MLP is independent of the generative model considered, and is trained with the generic truncated approximation (6). The idea of using a parametric function to approximate expectations w.r.t. intractable posteriors is an often applied technique. It goes back at least to wake-sleep approaches (Hinton et al., 1995) and has been used in different versions recently (Mnih and Gregor, 2014; Kingma and Welling, 2014; Rezende et al., 2014; Rezende and Mohamed, 2015; Mnih and Rezende, 2016).

For our numerical experiments we combine prior and (approximate) marginal sampling to suggest new variational states. The easy to use prior samplers are not data driven and represent rather an *exploration* strategy. Marginal sampling, on the other hand, is rather an *exploitation* strategy that produces good results when sufficiently much from the data is already known. Mixing the two has therefore turned out best for our purposes. Posterior samplers do require additional derivations but, to our experience so far, are also not necessarily better than combined prior and marginal sampling in optimizing the truncated free-energy.

Before we consider concrete generative models, let us summarize the general novel procedure in the form of the pseudo code given by Alg. 2. First, we have to initialize the model parameters Θ and the sets $\mathcal{K}^{(n)}$. While initializing Θ can be done as for other EM approaches, one option for an initialization of $\mathcal{K}^{(n)}$ would be the use of samples from the prior given Θ (more details are given below). The inner loop (the variational E-step) of Alg. 2 is then based on a mix of prior and marginal samplers, and each of these samplers is directly defined in terms of a considered generative model, no model-specific derivations are used. The same does not apply for the M-step but we will consider two examples how this point can be

Algorithm 2: Truncated Variational Sampling.

```

initialize model parameters  $\Theta$ ;
for all  $n$  init  $\mathcal{K}^{(n)}$  such that  $|\mathcal{K}^{(n)}| = S$ ;
set  $M_p$ ; (number of samples from prior distribution)
set  $M_q$ ; (number of samples from marginal distr.)
repeat
  update numbers  $M_p$  and  $M_q$ ;
  (sampler adjustment)
  for ( $n = 1, \dots, N$ ) do
    draw  $M_p$  samples from  $p(\vec{s} | \Theta) \rightarrow \mathcal{K}_p^{(n)}$ ;
    draw  $M_q$  samples from  $q_{\text{mar}}^{(n)}(\vec{s}; \Theta) \rightarrow \mathcal{K}_q^{(n)}$ ;
     $\mathcal{K}^{(n)} = \mathcal{K}^{(n)} \cup \mathcal{K}_p^{(n)} \cup \mathcal{K}_q^{(n)}$ ;
    remove those ( $|\mathcal{K}^{(n)}| - S$ ) elements  $\vec{s}$  in  $\mathcal{K}^{(n)}$ 
      with lowest  $p(\vec{s}, \bar{y}^{(n)} | \Theta)$ ;
   $\mathcal{K} = (\mathcal{K}^{(1)}, \dots, \mathcal{K}^{(N)})$ ;
  use M-steps with (2) to change  $\Theta$ ;
until parameters  $\Theta$  have sufficiently converged;

```

addressed: (A) either by using well-known standard M-step or (B) by applying automatic differentiation. Alg. 2 will be referred to as *truncated variational sampling* (TVS).

4 Applications of TVS

We study two types of generative models with binary latents: Binary Sparse Coding and Sigmoid Belief Networks. The models are complementary in many aspects, and thus serve well as example applications.

4.1 TVS for Binary Sparse Coding

In the first example we will consider dictionary learning – a typical application domain of variational EM approaches and sampling approaches in general. Probabilistic sparse coding models are not computationally tractable and common approximations such as maximum a-posteriori approximations (e.g. Olshausen and Field, 1996) can result in suboptimal solutions. Factored variational EM as well as sampling approaches have therefore been routinely applied to sparse coding. Of particular interest for our purposes are sparse

coding models with discrete and semi-discrete latents (e.g. Haft et al., 2004; Henniges et al., 2010; Goodfellow et al., 2012; Sheikh et al., 2014). These binary and ‘spike-and-slab’ approaches have been shown to perform well in many settings (Titsias and Lázaro-Gredilla, 2011; Goodfellow et al., 2012; Sheikh et al., 2014) as they seem to be better matched, e.g., to the statistics of natural images. We will here focus on elementary and linear binary sparse coding (e.g. Haft et al., 2004; Henniges et al., 2010; Bornschein et al., 2013) in order to highlight the applicability of TVS using a basic model. An application of the method to the more complex spike-and-slab data models would follow the same steps, however.

The BSC data model (Haft et al., 2004; Henniges et al., 2010) assumes independent and identically distributed (iid) binary latent variables following a Bernoulli prior distribution, and it uses a Gaussian noise model:

$$p(\vec{s} | \Theta) = \prod_{h=1}^H \pi^{s_h} (1 - \pi)^{1-s_h}, \quad \pi \in [0, 1], \quad (7)$$

$$p(\vec{y} | \vec{s}, \Theta) = \mathcal{N}(\vec{y}; W\vec{s}, \sigma^2 \mathbb{1}), \quad (8)$$

where $\Theta = (\pi, W, \sigma^2)$ is the set of model parameters.

TVS for BSC. As TVS is an approximate EM approach, let us first consider exact EM which seeks parameters Θ that optimize the data likelihood for the BSC data model (7) and (8). Parameter update equations are canonically derived and are given by (e.g. Henniges et al., 2010):

$$\pi = \frac{1}{N} \sum_{n=1}^N \sum_{h=1}^H \langle s_h \rangle_{q_n} \quad (9)$$

$$W = \left(\sum_{n=1}^N \vec{y}^{(n)} \langle \vec{s} \rangle_{q_n}^T \right) \left(\sum_{n=1}^N \langle \vec{s} \vec{s}^T \rangle_{q_n} \right)^{-1} \quad (10)$$

$$\sigma^2 = \frac{1}{ND} \sum_{n=1}^N \langle \|\vec{y}^{(n)} - W\vec{s}\|^2 \rangle_{q_n} \quad (11)$$

where the q_n are equal to the exact posteriors for exact EM, $q_n = p(\vec{s} | \vec{y}^{(n)}, \Theta)$.

A standard variational EM approach for BSC would now replace these posteriors by variational distributions q_n . Applications of (mean-field) variational distributions as, e.g., applied by Haft et al. (2004), entails (A) a choice which family of distributions to use; and (B) additional derivations in order to derive update equations for the introduced variational parameters. Also the derivation of sampling based approaches would require derivations. The same is not the case for the application of TVS (Alg. 2). In order to obtain a TVS learning algorithm for BSC, we do (for the update equations) just have to replace the expectation

values of the M-steps in Eqns. 9 to 11 by (2). For the E-step, we then use the generative model description (Eqns. 7 to 8) in order to update the sets $\mathcal{K}^{(n)}$ using prior and approximate marginal distributions as described by Alg. 2.

Numerical Experiments on Artificial Data.

Firstly, we verify and study the novel approach using artificial data generated by the BSC data model using ground-truth generating parameters Θ_{gt} . We use $H = 10$ latent variables, s_h , sampled independently by a Bernoulli distribution parameterized by $\pi_{gt} = 0.2$. We set the ground truth parameters for the dictionary matrix, $W \in \mathbb{R}^{D \times H}$ to appear like vertical and horizontal bars (compare Hoyer, 2002) when rasterized to 5×5 images, see Figure 1, with a value of 10 for a pixel that belongs to the bar and 0 for a pixel that belongs to the background. We linearly combine the latent variables with the dictionary elements to generate a $D = 25$ -dimensional datapoint, \vec{y} to which we add mean-free Gaussian noise with standard deviation $\sigma_{gt} = 2.0$. In this way we generate $N = 10\,000$ datapoints that form our artificial dataset. We now use TVS for BSC to fit another instance of the BSC model to the generated data. The model is initialized with a noise parameter σ equal to the average standard deviation of each observation in the data $\vec{y}^{(n)}$, the prior parameter is initialized as $\pi = 1/H$ were the latent variable $H = 10$ is maintained from the generating model. We initialize the columns of the dictionary matrix with the mean datapoint plus mean Gaussian samples with a standard deviation $\sigma/4$.

We train the model using the TVS algorithm for 200 TV-EM iterations maintaining the number of variational states at $|\mathcal{K}^{(n)}| = S = 64$ for all datapoints throughout the duration of the training. We use $M_q = 32$ samples drawn from the marginal distribution (only 1st approximation) and $M_p = 32$ samples drawn from the prior to vary \mathcal{K} according to Alg. 2. The evolution of the parameters during training is presented in Figure 1. We were able to extract very precise estimates of the ground truth parameters of the dataset. Convergence is faster for the dictionary elements W while we finally also achieve very good estimates for the noise scale σ and prior π . We also appear to achieve a very close approximation of the exact log-likelihood using the truncated free-energy (Fig. 1), which shows that our free-energy bound is very tight for this data.

Numerical Experiments on Image Patches. After verification, we then used the BSC data model trained with TVS to extract components of natural image patches, which is a standard task for sparse coding (Olshausen and Field, 1996). As dataset we use

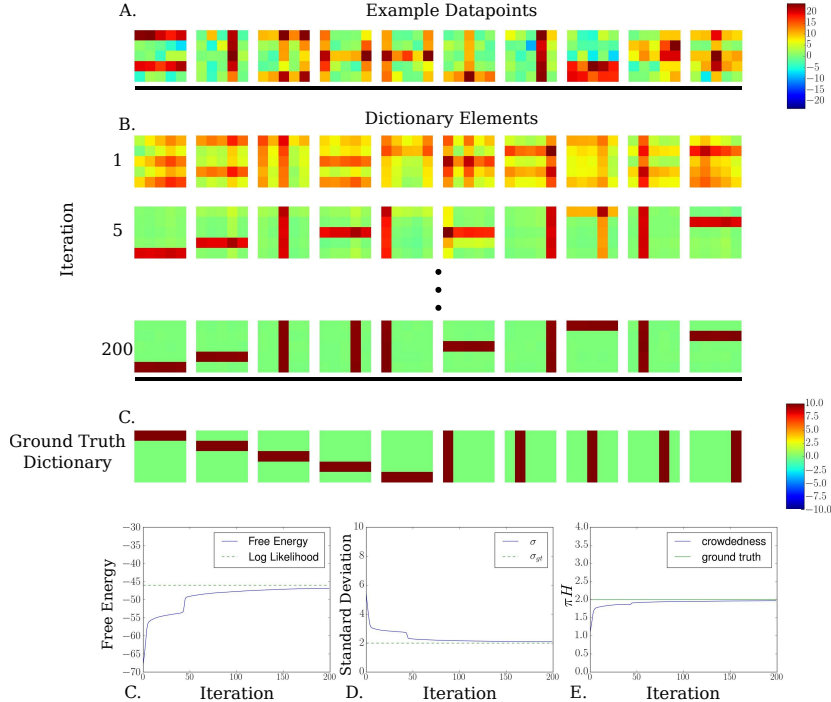


Figure 1: **Linear Bars Test.** **A.** A subset of the generated datapoints. **B.** The evolution of the dictionary over TVS iterations. Note that permutations of the dictionary elements would yield the same likelihood. **C.** The ground truth dictionary. **D.** The evolution of free-energy over TVS iterations plotted next to the exact log-likelihood. **E.** The evolution of the model standard deviation plotted next to the ground truth. **F.** The evolution of the expected number of active units πH plotted against the ground truth.

$N = 100\,000$ patches of size $D = 16 \times 16$ from a subset of the Van Hateren image dataset (van Hateren and van der Schaaf, 1998) that excludes images containing artificial structures. We preprocessed the images by whitening using the ZCA algorithm as described by Bell and Sejnowski (1997) retaining 95% of the variance. We used the resulting patches as input $\vec{y}^{(n)}$ for the algorithm. We trained the model with the TVS algorithm for 2000 EM iterations. We use a sampler adjustment (see Alg. 2) and used for the first 100 iterations of TV-EM $M_p = 200$ samples from the prior and $M_q = 0$ samples from the marginal distribution (only 1st approximation). From iteration 100 to iteration 200 we then linearly decreased the number of prior samples to $M_p = 0$ and increased the number of marginal samples to $M_q = 200$ such that at all times $M_p + M_q = 200$. Thus a sampler adjustment we observed to assist in avoiding early convergence to local optima. The resulting parameter development is shown in Fig. 2. As for artificial data we observed the basis functions (rows of W) to converge fast. Convergence of π and σ^2 was much slower (note their still final slopes after 2000 iterations). The basis functions converged to represent, e.g., Gabor functions (compare Olshausen and Field, 1996; Henniges et al., 2010; Bornschein et al., 2013). Applying also the 2nd MLP-based marginal approximation improved convergence times significantly (convergence within 200 iterations) but free-energy values were lower (presumably because the MLP resulted in less exploration).

4.2 TVS for Sigmoid Belief Networks

The second example we will consider here is a typical representative of a Bayesian Network: Sigmoid Belief Networks (SBNs; Saul et al., 1996). While sparse coding approaches are applied to continuous (Gaussian distributed) observed variables, SBNs have binary observed and hidden variables. A further difference is that SBNs require gradients for parameter updates (partial M-steps), while parameter updates of sparse coding models including BSC have well-known updates that fully maximize a corresponding free-energy (full M-steps). SBNs thus serve as an example complementary to BSC, and is well suited for our purposes of studying generality and effectiveness of TVS.

The SBN Model. An SBN has potentially many layers of latent variables but we will here maintain the same graphical model architecture as for BSC, i.e., an SBN with one observed and one hidden layer. The probability distribution for one SBN layer is given by:

$$p(\vec{y}|\vec{s}) = \prod_d g_d^{y_d} (1 - g_d)^{(1-y_d)} \quad (12)$$

where $g_d = \sigma(\sum_h W_{dh}s_h + b_d)$ and σ denotes the Sigmoid function. For the hidden layer, an SBN uses an independent prior distribution:

$$p(s_h) = \prod_h \pi_h^{s_h} (1 - \pi_h)^{(1-s_h)} \quad (13)$$

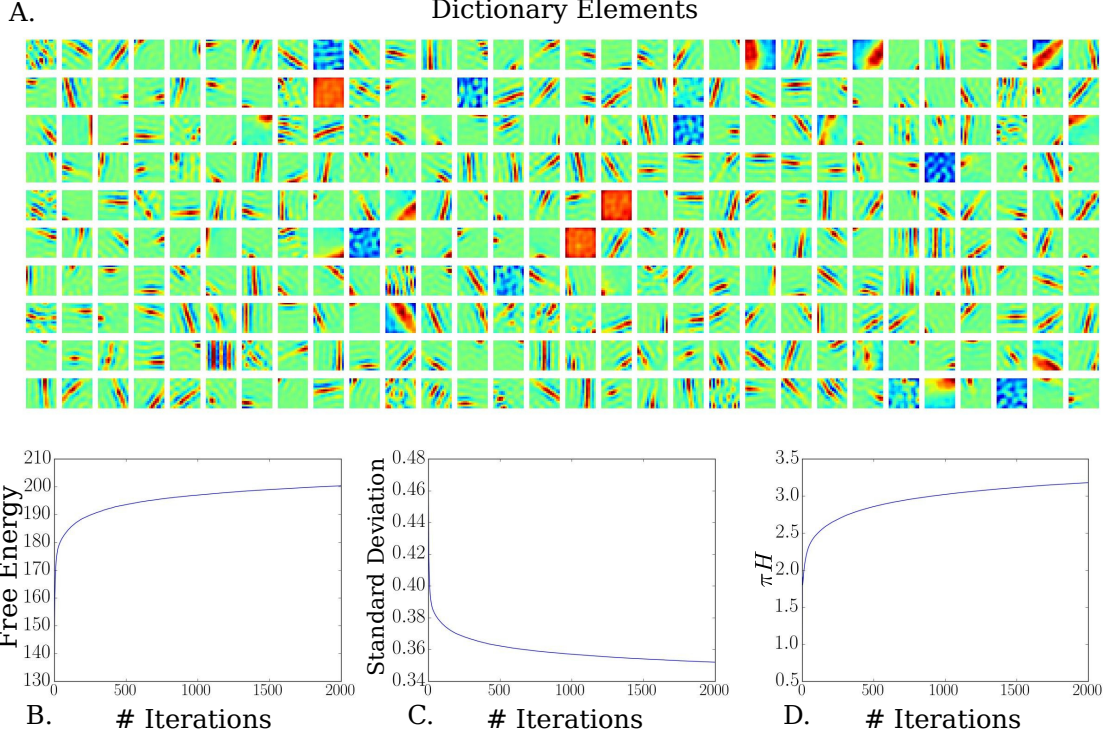


Figure 2: **Natural Image Statistics.** **A.** The dictionary at convergence. **B.** The evolution of the free-energy over TVS iterations. **C.** The evolution of the model standard deviation over TVS iterations. **E.** Evolution of the expected number of active units πH over TVS iterations. Please enlarge for better visibility.

where π_h parameterizes the prior distribution. In general, inference for SBNs is challenging because of its binary latent variables which can show complex dependencies. Because of this, direct applications of standard variational approaches (e.g. Saul et al., 1996) are challenging, and also popular recent variational methods applying reparameterization (Kingma and Welling, 2014; Rezende et al., 2014) are not directly applicable. Also (variational) sampling approaches require additional mechanisms, e.g., the score function based approach needs to reduce the variance of estimation (Mnih and Gregor, 2014).

TVS for SBNs. Let us now study what is required to device a TVS algorithm for SBNs. As for BSC, it is straightforward to apply TVS for optimizing SBNs. We define a truncated latent space $\mathcal{K}^{(n)}$ for the latent vector \vec{s} . Then, Alg. 2 can be directly used as it only requires to compute the joint log probability in order to generate samples from the prior and approximate marginal distributions.

Numerical Experiments on Artificial Data. Like for BSC, we first apply our method on a classical small scale problem, where the true likelihood is still tractable. The generation of the dataset is similar to the linear bars test mentioned in the above section,

where the difference is that, in this case, the resulting representations go through the sigmoid function and produce binary representations (i.e., we generate according to an SBN model). A few generated examples (of $N = 2000$ used) are shown in Fig. 3A. We apply a sigmoid belief network with $H = 10$ hidden units. As for BSC, we use for this small scale experiment a distribution $q_{\text{mar}}^{(n)}(\vec{s}; \Theta)$ according to the 1st approximation of the marginal probability. We used $|\mathcal{K}^{(n)}| = S = 50$ and very few samples for variation were found sufficient ($M_q = M_p = 5$). The learning curve of the free energy in (3) of a typical run is shown in Fig. 3C. As can be observed, the free-energy monotonically increases undergoing some “phase transitions”. Note that, at the end of learning, the free-energy surpasses the log-likelihood of the generating parameters because of the limited size of training data (slight overfitting). After convergence, the learned weight matrix W of the hidden layer is visualized in Figure 3B. It can be observed that all “bars” are represented.

Numerical Experiments on Binarized MNIST. Finally, we apply TVS for SBN with different numbers of latents, and evaluate its performance on the

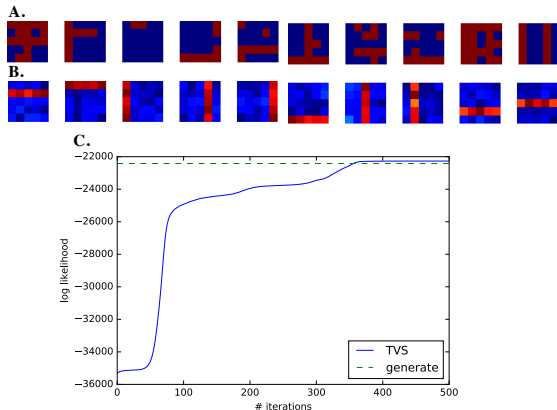


Figure 3: Application of a shallow SBN with TVS to synthetic data (bars test). **A** Ten examples of the training data points. **B** Visualization of the learned weight matrix W of the shallow SBN. All bars are discovered, one for each hidden unit. **C** Learning curve of the free energy. The dashed green line shows the true log likelihood of the SBN with the parameters used for generating the training data.

Binarized MNIST dataset¹. We set $|\mathcal{K}^{(n)}| = S = 50$, $M_p = 10$, $M_q = 20$ and keep M_p, M_q constant for all our experiments. For these larger scale applications, SBN optimization was observed to be significantly faster if the second marginal approximation for $q_{\text{mar}}^{(n)}(\vec{s}; \Theta)$ was applied. In the following we, therefore, report results for truncated marginal distributions approximated using an MLP with one hidden layer of 500 hidden units and \tanh activation. The standard performance measure for SBNs on Binarized MNIST is the average log-likelihood on the test data. The likelihood often has to be estimated with considerable additional effort (Bornschein and Bengio, 2015; Hjelm et al., 2016, use Monte Carlo integration, for instance). For TVS we can use the truncated free-energy bound as estimate which is available without additional effort and given by iterating the TV-E-steps of Alg. 2 using the test data. No sampler adjustment is used (constant M_p and M_q throughout learning). The resulting performance comparison is shown in Table 1. Note that the shown test log-likelihood of our method is a variational lower bound of our learned log-likelihood, where the results by Bornschein and Bengio (2015); Hjelm et al. (2016) are from Monte Carlo estimations (which may lie a bit above or below the true value). For SBNs with 200 hidden units, we observed that TVS slightly outperforms NVIL, and its performance is comparable to RWS. The results of Gan et al. (2015) can not di-

¹Downloaded from (Larochelle, 2011), which was converted according to (Murray and Salakhutdinov, 2008).

Table 1: Results on the binarized MNIST dataset. “dim” is the number of latent variables for each approach (starting with the deepest one for models with two layers). (*) taken from (Gan et al., 2015), (\diamond) taken from (Mnih and Gregor, 2014), (\dagger) taken from (Bornschein and Bengio, 2015), (\ddagger) taken from (Hjelm et al., 2016).

model	dim	test log-prob.
SBN (TVS)	100	-121.91
SBN (TVS)	200	-111.23
SBN (Gibbs)*	200	-94.3
SBN (VB)*	200	-117.0
SBN (NVIL) \diamond	200	-113.1
SBN (NVIL) \diamond	200-200	-99.8
SBN (WS) \dagger	200	-120.7
SBN (WS) \dagger	200-200	-109.4
SBN (RWS) \dagger	200	-103.1
SBN (RWS) \dagger	200-200	-93.4
SBN (AIR) \ddagger	200	-100.9
SBN (AIR) \ddagger	200-200	-92.9

rectly serve as a comparison of variational approaches, as additional sparse priors (additional knowledge) on the network weights are used.

5 Discussion

Variational EM and sampling represent two classes of approximations that are applied to efficiently train probabilistic generative models; and their combination has been proven beneficial in many applications. BBVI (Ranganath et al., 2014), for instance, uses mean-field variational distributions and subsequently draws samples of the variational distribution to estimate expectation values for parameter updates. Other approaches seek to overcome the limitations of mean-field (i.e., its assumed a-posteriori independence) by using, e.g., *reparameterization* of mean-field approaches (Kingma and Welling, 2014; Rezende et al., 2014), *normalizing flow* (Rezende and Mohamed, 2015) or truncated posteriors (Shelton et al., 2011; Sheikh and Lücke, 2016); also compare (Tran et al., 2015; Rezende and Mohamed, 2015; Bornschein and Bengio, 2015; Hjelm et al., 2016; Kucukelbir et al., 2016). Ranganath et al. (2016) extended *normalizing flow* to handle discrete latent variables by additionally lower bounding the variational objectives. NVIL followed a similar idea but used an MLP to model the variational distribution (Mnih and Gregor, 2014).

The TVS approach studied here is different from all these previous approaches: it does *not* rely on a para-

metric form of a variational distribution which is then sampled from to estimate parameter updates. In contrast, for TVS, the drawn samples *themselves* define the variational distribution and act as its variational parameters. Changing the used samples changes the variational distribution. TVS is thus by definition directly coupling sampling and variational EM. This novel combination and the ‘black box’ applicability which follows are the main contributions of this study. A benefit of the tight coupling seems to be that none of the diverse variance reduction techniques (which were central to BBVI or NVIL) are required. TVS can thus be considered as the most directly applicable ‘black box’ approach. On the other hand, TVS was here only applied to SBNs with the same architecture as BSC (one observed and one hidden layer). Furthermore, TVS also required additional methods such as the use of a parameteric function (our 2nd approximation which applied an MLP). Such techniques were here observed to speed-up training times. In general, convergence times do depend on the quality of the samples a procedure suggests. If new samples which increase the free-energy are not found sufficiently frequently, learning becomes slow. Our MLP approach improved convergence times but so can do other procedures or refined sampling distributions. Future work will, therefore, investigate further enhancements of sampling and algorithmic improvements, while the general purpose property of TVS will be maintained. Moreover, further generative models will be investigated including those defined using more intricate graphical models.

Appendix Material

A The Truncated Variational EM Meta-Algorithm

If we consider the truncated distributions (1) as variational distributions, let us first treat all its parameters as variational parameters, i.e., the states $\mathcal{K}^{(n)}$ as well as its parameters Θ (which we will denote by $\hat{\Theta}$).

$$\begin{aligned} q^{(n)}(\vec{s}) &:= q^{(n)}(\vec{s}; \mathcal{K}, \hat{\Theta}) \\ &= \frac{p(\vec{s}, \vec{y}^{(n)} | \hat{\Theta})}{\sum_{\vec{s}' \in \mathcal{K}^{(n)}} p(\vec{s}', \vec{y}^{(n)} | \hat{\Theta})} \delta(\vec{s} \in \mathcal{K}^{(n)}). \end{aligned} \quad (14)$$

The variational paramters $\hat{\Theta}$ are of the same type as the model parameters Θ but may have different values. The variational distributions (14) define a correspond-

ing free-energy, which is given by:

$$\begin{aligned} \mathcal{F}(\mathcal{K}, \hat{\Theta}, \Theta) &= \sum_{n=1}^N \left(\sum_{\vec{s}} q^{(n)}(\vec{s}; \mathcal{K}, \hat{\Theta}) \log(p(\vec{s}, \vec{y}^{(n)} | \Theta)) \right) \\ &\quad + H(q(\vec{s}; \mathcal{K}, \hat{\Theta})), \end{aligned} \quad (15)$$

where $H(q)$ is an entropy term in which Θ is held fixed at $\hat{\Theta}$.

In order to show that the free-energy (15) has the form familiar from other variational EM approaches, and to formally show that it is a lower bound of the log-likelihood, the free-energy framework was extended by Lücke (2016) to also include variational distributions with exact (‘hard’) zeros (note that $q(\vec{s}) > 0$ is the standard requirement otherwise).

The standard functional form of (15) means that optimization of the free-energy w.r.t. Θ will take the same form as optimization w.r.t. full posteriors or any other variational approximations. Only the expectation values have to be taken w.r.t. $q^{(n)}(\vec{s}; \mathcal{K}, \hat{\Theta})$.

For the variational E-step, we have to optimize the variational parameters $\hat{\Theta}$ and \mathcal{K} . Regarding the optimization w.r.t. $\hat{\Theta}$ it can be shown (Lücke, 2016) that setting $\hat{\Theta} = \Theta$ maximizes the free-energy (15). Equating $\hat{\Theta} = \Theta$ is familiar from the free-energy formulation of exact EM (Lemma 1 of Neal and Hinton, 1998), where a full posterior can be regarded as variation approximation $q^{(n)}(\vec{s}; \hat{\Theta}) = p(\vec{s} | \vec{y}^{(n)}, \hat{\Theta})$. The proof that the same applies for truncated distributions (14) is a non-trivial generalization of this earlier observation (the full posterior case is recovered if we choose $\mathcal{K}^{(n)}$ to include all possible hidden states in which case the truncated distribution becomes equal to the full posterior, and the free-energy becomes equal to the standard form of exact EM).

As $\hat{\Theta} = \Theta$ maximizes the free-energy w.r.t. Θ , the non-trivial part of the variational E-step consist of maximizing (or increasing) the free-energy w.r.t. \mathcal{K} . If we first set $\hat{\Theta} = \Theta$, the free-energy (15) can first be simplified (Lücke, 2016) to take the form (3). The complete variational EM algorithm with partial E-step can then be formulated in the following form:

E-Step: choose \mathcal{K}_{new} such that

$$\mathcal{F}(\mathcal{K}_{\text{new}}, \Theta^{\text{old}}) \geq \mathcal{F}(\mathcal{K}_{\text{old}}, \Theta^{\text{old}})$$

M-Step: choose Θ^{new} such that

$$\mathcal{F}(\mathcal{K}_{\text{new}}, \Theta^{\text{old}}, \Theta^{\text{new}}) \geq \mathcal{F}(\mathcal{K}_{\text{new}}, \Theta^{\text{old}}, \Theta^{\text{old}})$$

Reset: $\mathcal{K}_{\text{old}} = \mathcal{K}_{\text{new}}, \Theta^{\text{old}} = \Theta^{\text{new}}$

(16)

Iterating (16) monotonously increases the truncated free-energy (3).

B Optimality of Algorithm 1

Consider the set $\mathcal{K}_{\text{old}}^{(n)}$ of size S united with the set $\mathcal{K}_{\text{new}}^{(n)}$ which contains M newly sampled state. The union of the two, $\mathcal{U}^{(n)} = \mathcal{K}_{\text{old}}^{(n)} \cup \mathcal{K}_{\text{new}}^{(n)}$, then contains at most $S + M$ states. We now want to find the subset $\tilde{\mathcal{K}}^{(n)} \subseteq \mathcal{U}^{(n)}$ of size S which results in the largest free-energy (3). Let us consider all other sets $\mathcal{K}^{(n)}$ of \mathcal{K} to be fixed, then the optimization problem to solve is by using (3) given as follows:

$$\tilde{\mathcal{K}}^{(n)} = \operatorname{argmax}_{\mathcal{K}^{(n)} \subseteq \mathcal{U}^{(n)}} \left\{ \sum_{\vec{s} \in \mathcal{K}^{(n)}} p(\vec{s}, \vec{y}^{(n)} | \Theta) \right\}, \text{ with } |\mathcal{K}| = S. \quad (17)$$

The optimization problem is solved if we define:

$$\begin{aligned} &\text{for all } \vec{s} \in \tilde{\mathcal{K}}^{(n)} \text{ and } \vec{s}' \notin \tilde{\mathcal{K}}^{(n)} : \\ &p(\vec{s}, \vec{y}^{(n)} | \Theta) \geq p(\vec{s}', \vec{y}^{(n)} | \Theta). \end{aligned} \quad (18)$$

In other words, if we pick the S states in $\mathcal{U}^{(n)}$ which have the largest joint values.

To see this observe that the objective in (17) with $\tilde{\mathcal{K}}^{(n)}$ is decreased whenever an arbitrary $\vec{s} \in \tilde{\mathcal{K}}^{(n)}$ is replaced by an $\vec{s}' \notin \tilde{\mathcal{K}}^{(n)}$. Hence, as no state \vec{s} can be found that improves the objective in (17), $\tilde{\mathcal{K}}^{(n)}$ represents the maximum. As the free-energy is a sum of N objectives (17), the set $\tilde{\mathcal{K}} = (\tilde{\mathcal{K}}^{(1)}, \dots, \tilde{\mathcal{K}}^{(N)})$ with $\tilde{\mathcal{K}}^{(n)}$ defined by (18) maximizes the free-energy (3).

Computing a set $\tilde{\mathcal{K}}^{(n)}$ requires to solve a partial sorting problem (finding the S largest elements in a list of all joints of the states in $\mathcal{U}^{(n)}$). If we take the list contains $|\mathcal{U}^{(n)}|$ values, the partial sorting problem can be solved with a time-complexity $\mathcal{O}(|\mathcal{U}^{(n)}|)$ (Blum et al., 1973). In our case, the list (the states in $\mathcal{U}^{(n)}$) contains at most $S + M$ elements. If the sets $\mathcal{K}_{\text{old}}^{(n)}$ and $\mathcal{K}_{\text{new}}^{(n)}$ have a non-zero intersection, $|\mathcal{U}^{(n)}|$ is smaller than $S + M$. In practice, $|\mathcal{U}^{(n)}|$ will be often only slightly larger than S (especially close to the end of learning), such that it is more efficient to remove the elements of $\mathcal{U}^{(n)}$ with the $(|\mathcal{U}^{(n)}| - S)$ lowest joints (which represents an equivalent partial sorting problem).

References

- Bell, A. J. and Sejnowski, T. J. (1997). The ‘independent components’ of natural scenes are edge filters. *Vision Research*, 37(23):3327–38.
- Blum, M., Floyd, R. W., Pratt, V., Rivest, R. L., and Tarjan, R. E. (1973). Time bounds for selection. *Journal of computer and system sciences*, 7(4):448–461.
- Bornschein, J. and Bengio, Y. (2015). Reweighted wake-sleep. In *ICLR*.
- Bornschein, J., Henniges, M., and Lücke, J. (2013). Are V1 receptive fields shaped by low-level visual occlusions? A comparative study. *PLOS Computational Biology*, 9(6):e1003062.
- Dai, Z. and Lücke, J. (2014). Autonomous document cleaning – a generative approach to reconstruct strongly corrupted scanned texts. *IEEE Transactions on Pattern Analysis and Machine Intelligence*, 36(10):1950–1962.
- Dempster, A. P., Laird, N. M., and Rubin, D. B. (1977). Maximum likelihood from incomplete data via the EM algorithm (with discussion). *Journal of the Royal Statistical Society B*, 39:1–38.
- Forster, D. and Lücke, J. (2017). Truncated variational EM for semi-supervised Neural Simpletrons. In *International Joint Conference on Neural Networks (IJCNN)*, pages 3769–3776.
- Gan, Z., Heno, R., Carlson, D., and Carin, L. (2015). Learning Deep Sigmoid Belief Networks with Data Augmentation. In *AISTATS*.
- Goodfellow, I., Courville, A. C., and Bengio, Y. (2012). Large-scale feature learning with spike-and-slab sparse coding. In *ICML*.
- Haft, M., Hofman, R., and Tresp, V. (2004). Generative binary codes. *Pattern Anal Appl*, 6:269–84.
- Henniges, M., Puertas, G., Bornschein, J., Eggert, J., and Lücke, J. (2010). Binary sparse coding. In *Proceedings LVA/ICA*, LNCS 6365, pages 450–57. Springer.
- Henniges, M., Turner, R. E., Sahani, M., Eggert, J., and Lücke, J. (2014). Efficient occlusive components analysis. *Journal of Machine Learning Research*, 15:2689–2722.
- Hernandez-Lobato, J., Li, Y., Rowland, M., Bui, T., Hernandez-Lobato, D., and Turner, R. (2016). Black-box alpha divergence minimization. In *International Conference on Machine Learning*, pages 1511–1520.
- Hinton, G. E., Dayan, P., Frey, B. J., and Neal, R. M. (1995). The ‘wake-sleep’ algorithm for unsupervised neural networks. *Science*, 268:1158 – 1161.
- Hjelm, R. D., Cho, K., Chung, J., Salakhutdinov, R., Calhoun, V., and Jovic, N. (2016). Iterative refinement of the approximate posterior for directed belief networks. In *NIPS*.

- Hoffman, M. D., Blei, D. M., Wang, C., and Paisley, J. W. (2013). Stochastic variational inference. *Journal of Machine Learning Research*, 14(1):1303–1347.
- Hoyer, P. O. (2002). Non-negative sparse coding. In *Neural Networks for Signal Processing XII: Proceedings of the IEEE Workshop on Neural Networks for Signal Processing*, pages 557–65.
- Hughes, M. C. and Sudderth, E. B. (2016). Fast learning of clusters and topics via sparse posteriors. *arXiv preprint arXiv:1609.07521*.
- Ilin, A. and Valpola, H. (2005). On the effect of the form of the posterior approximation in variational learning of ICA models. *Neural Processing Letters*, 22(2):183–204.
- Jordan, M., Ghahramani, Z., Jaakkola, T., and Saul, L. (1999). An introduction to variational methods for graphical models. *Machine Learning*, 37:183–233.
- Kingma, D. P. and Welling, M. (2014). Auto-encoding variational bayes. In *ICLR*.
- Kucukelbir, A., Tran, D., Ranganath, R., Gelman, A., and Blei, D. M. (2016). Automatic differentiation variational inference. *CoRR*, abs/1603.00788.
- Larochelle, H. (2011). Binarized mnist dataset. <http://www.cs.toronto.edu/~larocheh/>.
- Lücke, J. (2016). Truncated variational expectation maximization. *arXiv preprint, arXiv:1610.03113*.
- Lücke, J. and Eggert, J. (2010). Expectation truncation and the benefits of preselection in training generative models. *Journal of Machine Learning Research*, 11:2855–900.
- Lücke, J. and Forster, D. (2017). k-means is a variational EM approximation of Gaussian mixture models. *arXiv preprint arXiv:1704.04812*.
- Lücke, J. and Sahani, M. (2008). Maximal causes for non-linear component extraction. *Journal of Machine Learning Research*, 9:1227–67.
- MacKay, D. J. C. (2003). *Information Theory, Inference, and Learning Algorithms*. Cambridge University Press. Available from <http://www.inference.phy.cam.ac.uk/mackay/itila/>.
- Mnih, A. and Gregor, K. (2014). Neural variational inference and learning in belief networks. In *Proceedings of The 31st International Conference on Machine Learning*.
- Mnih, A. and Rezende, D. J. (2016). Variational inference for monte carlo objectives. In *ICML*.
- Murray, I. and Salakhutdinov, R. (2008). Evaluating probabilities under high-dimensional latent variable models. In *NIPS*.
- Neal, R. and Hinton, G. (1998). A view of the EM algorithm that justifies incremental, sparse, and other variants. In Jordan, M. I., editor, *Learning in Graphical Models*. Kluwer.
- Olshausen, B. and Field, D. (1996). Emergence of simple-cell receptive field properties by learning a sparse code for natural images. *Nature*, 381:607–9.
- Ranganath, R., Gerrish, S., and Blei, D. M. (2014). Black box variational inference. In *AISTATS*, pages 814–822.
- Ranganath, R., Tran, D., and Blei, D. M. (2016). Hierarchical variational models. In *International Conference on Machine Learning*.
- Rezende, D. J. and Mohamed, S. (2015). Variational inference with normalizing flows. *International Conference on Machine Learning*.
- Rezende, D. J., Mohamed, S., and Wierstra, D. (2014). Stochastic backpropagation and approximate inference in deep generative models. In *ICML*.
- Salimans, T., Kingma, D. P., Welling, M., et al. (2015). Markov chain monte carlo and variational inference: Bridging the gap. In *International Conference on Machine Learning*, pages 1218–1226.
- Saul, L. K., Jaakkola, T., and Jordan, M. I. (1996). Mean field theory for sigmoid belief networks. *Journal of artificial intelligence research*, 4(1):61–76.
- Sheikh, A.-S. and Lücke, J. (2016). Select-and-sample for spike-and-slab sparse coding. In *Advances in Neural Information Processing Systems (NIPS)*, volume 29, pages 3927–3935.
- Sheikh, A.-S., Shelton, J. A., and Lücke, J. (2014). A truncated EM approach for spike-and-slab sparse coding. *Journal of Machine Learning Research*, 15:2653–2687.
- Shelton, J. A., Bornschein, J., Sheikh, A.-S., Berkes, P., and Lücke, J. (2011). Select and sample – a model of efficient neural inference and learning. *Advances in Neural Information Processing Systems*, 24:2618–2626.

- Shelton, J. A., Gasthaus, J., Dai, Z., Lücke, J., and Gretton, A. (2017). Gp-select: Accelerating em using adaptive subspace preselection. *Neural Computation*, 29(8):2177–2202.
- Titsias, M. K. and Lázaro-Gredilla, M. (2011). Spike and slab variational inference for multi-task and multiple kernel learning. In *NIPS*, volume 24.
- Tran, D., Blei, D., and Airoldi, E. M. (2015). Copula variational inference. In *Advances in Neural Information Processing Systems*, pages 3564–3572.
- Turner, R. E. and Sahani, M. (2011). *Bayesian Time Series Models*, chapter Two problems with variational expectation maximisation for time-series models. Cambridge University Press.
- van Hateren, J. H. and van der Schaaf, A. (1998). Independent component filters of natural images compared with simple cells in primary visual cortex. *Proceedings of the Royal Society of London B*, 265:359–66.